Spectral response of Different Combustion Models in LES of Direct Combustion Noise

F. Zhang*, T. Zirwes, H. Nawroth***, N. Li*, P. Habisreuther*, H. Bockhorn*, D. Trimis*, C.O. Paschereit*****

Feichi.Zhang@kit.edu

* Engler-Bunte-Institute, Division of Combustion Technology, Karlsruhe Institute of Technology, Engler-Bunte-Ring 1, 76131 Karlsruhe, Germany

** Steinbuch Centre for Computing (SCC), Karlsruhe Institute of Technology, Hermann-von-Helmholtz-Platz 1, Karlsruhe, Germany

*** Institute of Fluid Dynamics and Technical Acoustics, Technische Universität Berlin,Müller-Breslau-Straße 8, 10623 Berlin, Germany

Abstract

This work presents compressible large eddy simulation (LES) of a turbulent premixed methane/air jet flame along with two commonly used combustion models, the turbulent flame-speed closure (TFC-class) and the dynamically thickened flame (DTF) model. The mean and rms statistics of the flow velocity calculated with both TFC and DTF models show a reasonable agreement. However, DTF-LES predicts a higher sound pressure level compared to the TFC-LES, the reason is that the flame is thinner in the DTF-LES compared to TFC-LES, leading to a stronger flame-turbulence interaction and heat release rate fluctuation. In the DTF model, mean reaction rates are based on an Arrhenius-like model, whereas the current implementation of the TFC model postulates the mean rate as a parabolic function of the reaction progress variable. The difference between sound spectra calculated with DTF- and TFC-LES has been found to be dependent on the frequency range. The dependence is weak in the low and high frequency range and large in an intermediate range. This reflects the different spectral response behavior of TFC and DTF models to turbulent flow, which is essential when using compressible LES for calculating thermo-acoustics such as combustion noise.

1. Introduction

The reduction of noise emission has become an increasing important issue for industrial combustion devices such as aircraft engines or gas turbines [1, 2]. In low-Mach number flows, the transient fluctuations of the local heat release rate due to flame-turbulence interactions represent the main source of noise, which is known as direct combustion noise. Its generation mechanism is described by the unsteady generation of gas volume through thermal expansion, which leads to a temporal density fluctuation. Direct combustion noise exhibits a broadband distribution in the spectral domain, which correlates to the spectrum of turbulent kinetic energy due to the mutual interaction between heat release and turbulent fluctuations [3, 4]. Computational fluid dynamics (CFD) is widely used to study

combustion noise and its formation mechanisms. Among the different CFD approaches, the LES technique is viewed as a compromise between computing effort and accuracy and has found widespread use for the simulation of combustion and combustion noise in the last decade [2, 4, 5]. A variety of combustion models exists [6, 7, 8], where the treatment of flame-turbulence interactions is described with different physical aspects. For example, the level-set approach [7, 8] is derived by assuming an infinitely thin flame and tracking solely the dynamic movement of the respective flame surface due to the turbulent flow and flame's propagation. In the artificially thickened flame model [9], the flame is thickened in order to resolve it on a coarse grid. Therefore, the resolved flame structure as well as its response to the turbulent flow are affected by using different modeling concepts. The effects and consequences of two commonly used combustion models on noise formation will be demonstrated here by means of LES of a premixed turbulent jet flame.

2. Combustion Modeling

2.1 Turbulent Flame-speed Closure (TFC) Model

For the current implementation of the TFC class model, a transport equation for the Favre-filtered progress variable $\tilde{c}$ is solved [4]:

$$\frac{\partial \bar{\rho}\,\widetilde{c}}{\partial t} + \frac{\partial \bar{\rho}\tilde{u}_i\,\widetilde{c}}{\partial x_i} = \frac{\partial}{\partial x_i}\left(\frac{\mu_l + \mu_t}{Sc_t}\frac{\partial\,\widetilde{c}}{\partial x_i}\right) + \bar{\dot{\omega}}_c \qquad (1)$$

where $\bar{\cdot}$ denotes a filtered and $\tilde{\cdot}$ a Favre-filtered value. μ_l and μ_t are the laminar and turbulent viscosity. Sc_t is the turbulent Schmidt number. Focus of the model is to represent the source term $\bar{\dot{\omega}}_c$ with the turbulent flame speed S_t, which considers the effect of flame-turbulence interactions [10]:

$$\bar{\dot{\omega}}_c = \rho_0 \frac{S_t^2}{D_l + D_t}\,\widetilde{c}\,(1 - \widetilde{c}), \qquad \frac{S_t}{S_l} = \frac{u'}{S_l}\left(1 + {D_a}^{-2}\right)^{-\frac{1}{4}} \qquad (2)$$

ρ_0 is the density of the unburnt gas, S_l the unstretched laminar flame speed, u' the turbulence intensity, D_l and D_t the laminar and turbulent diffusivity. The Damköhler number Da is evaluated by the ratio of turbulent to chemical time scales $D_a = \tau_t/\tau_c \propto (L_t/u')/(a_0/S_l^2)$ with the turbulent length scale L_t and the thermal diffusivity of the unburnt gas a_0. In the context of LES modeling, the turbulence parameters u', L_t, $D_t = u' \cdot L_t$ are calculated from the sub-grid scale turbulence model. S_t represents in this case an effective burning velocity, which depends on the grid resolution. Structures of the flame zones are pre-computed by simulating unstrained 1D flames. The species mass fractions are then projected onto the c-space. In this work, c is calculated with the chemically bound oxygen.

2.2 Dynamically Thickened Flame (DTF) Model

The DTF model is based on thickening the actual flame front artificially while keeping the flame speed constant [9, 11]. It also introduces an efficiency parameter to account for the attenuated flame-turbulence interactions caused by a reduced Da

through the thickening procedure. A transport equation is solved for each species:

$$\frac{\partial \bar{\rho}\tilde{Y}_k}{\partial t} + \frac{\partial \bar{\rho}\tilde{u}_i\tilde{Y}_k}{\partial x_i} = \frac{\partial}{\partial x_i}\left((EF\frac{\mu_l}{Sc_k})\frac{\partial \tilde{Y}_k}{\partial x_i}\right) + \frac{E}{F}\bar{\dot{\omega}}_k \quad (3)$$

where $\tilde{Y}_k$ is the Favre-filtered mass fraction and Sc_k the Schmidt number of the *k*-th species. The filtered mean reaction rate $\bar{\dot{\omega}}_k$ is evaluated from the reaction rates of the respective species with the rate coefficient is given by an Arrhenius temperature dependency. The thickening factor F and the efficiency factor E are given by [9, 11]:

$$F = max\left(\frac{n\Delta}{\delta_l}, 1\right), \qquad E = \frac{1 + \alpha\Gamma\left(\frac{\Delta_e}{\delta_l}, \frac{u'}{S_l}\right)\frac{u'}{S_l}}{1 + \alpha\Gamma\left(\frac{\Delta_e}{\delta_l^1}, \frac{u'}{S_l}\right)\frac{u'}{S_l}} \quad (4)$$

with the grid size Δ, the laminar flame thickness δ_l and n the number of grid cells used to resolve the thickened flame. The computation of F is only active within the reaction zone and F is equal to 1 elsewhere. E takes into account the increase of mean reaction rates due to turbulent fluctuations, for example, through wrinkling of the flame surface. Γ indicates a functional operator and Δ_e the local filter size. δ_l^1 is the resolved flame thickness, i.e., $\delta_l^1 = F\delta_l = n\Delta$. α is a model constant that scales with $Re^{-1/2}$. The required turbulence parameters in both TFC and DTF models like u' and L_t are evaluated from the sub-grid turbulence modeling.

3. Numerical Setup

The above described methods are applied to a turbulent premixed methane/air jet flame operated at atmospheric conditions ($T_0 = 293$ K, $p_0 = 1$ atm) [12, 13], using two equivalence ratios $\phi = 0.7$ and $\phi = 0.9$. The Reynolds number based on the nozzle diameter D and the bulk velocity is $Re = 15{,}000$. The computational domain consists of the convergent nozzle part and a large cylindrical domain with an extension of 80 D in axial and radial direction, containing approx. 11.2 million hexahedral grid cells. The grid is systematically refined along the burner wall and the shear layer with a smallest grid size of 0.3 mm.

OpenFOAM [14] has been used to solve the governing equations with the finite volume method in a fully implicit compressible formulation [15]. We implemented the TFC and DTF models described in Sec.2 into this code. For the DTF model, $n = 2.5$ is used to resolve the flame, along with a two-step reaction mechanism and prescribed Sc_k for each species individually [11]. The GRI-3.0 [16] mechanisms is used for the chemistry tabulation in the TFC model. The Smagorinsky Model [17] has been used for sub-grid scale (SGS) turbulence modeling.

4. Results

Figure 1 shows instantaneous (left) and time-mean (right) contours of temperature calculated from LES using the TFC and the DTF model for the case of $\phi = 0.9$. The resolved flame is thinner and more heavily wrinkled with DTF compared to

TFC. This is attributed to the evaluation of the mean reaction rates by a parabolic shape-function $\widetilde{c}\,(1-\widetilde{c}\,)$ in the TFC model (see Eq.(2)). This approach alters the internal flame structure by broadening the evolution of $\overline{\dot{\omega}}_c$ spatially. For the DTF model, the flame thickness is prescribed by the thickening factor and the reaction rate is evaluated with the kinetic rate expression scaled by E/F (see Eq.(3)), which results in a thinner flame and hence, a more intense flame-turbulence interaction compared to the TFC model.

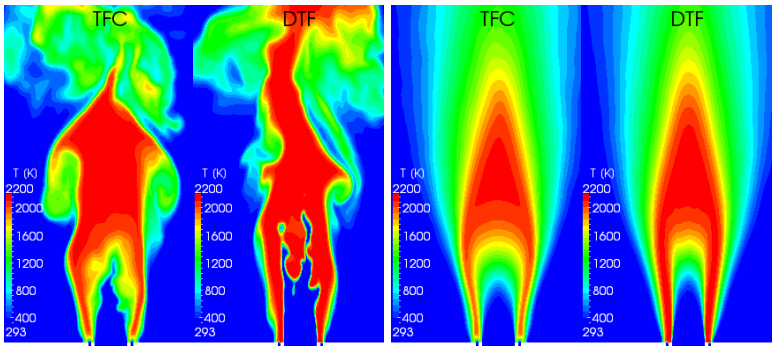

Figure 1. Comparison of instantaneous (left) and (right) time-mean temperature calculated with TFC and DTF combustion models.

In Fig.2, the time mean and root mean square (rms) values of the axial and radial velocities calculated with TFC and DTF are compared with experimental data for different streamwise locations: $x/D = 0.4$ to $x/D = 4$. The mean values (1st and 2nd column) obtained from TFC and DTF show a good agreement and also compare well to the measured data. The predicted resolved rms values (3rd and 4th column) are however higher in DTF-LES compared with TFC-LES. This is due to the resolved thinner flame by the DTF-LES compared to TFC-LES, which leads to a stronger wrinkling of the flame surface and fluctuation of velocity at the flame front.

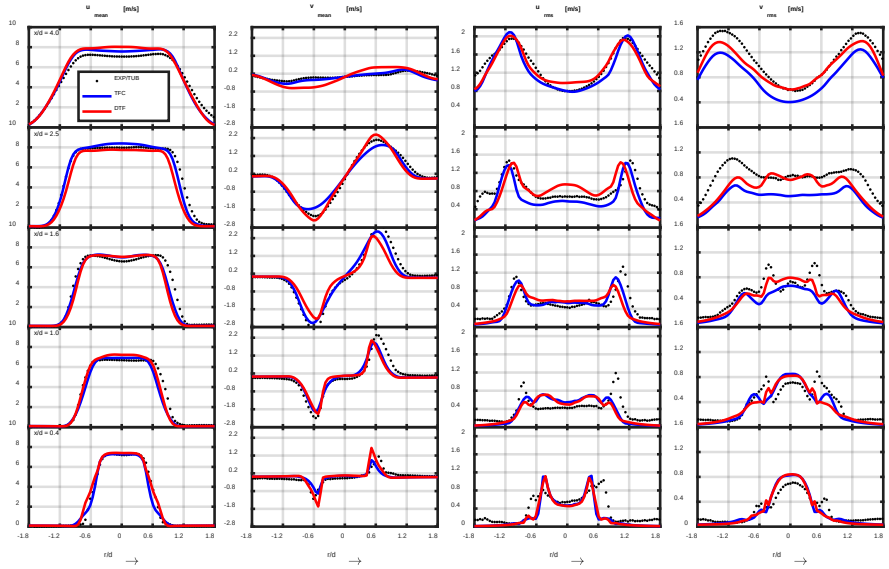

Figure 2. Comparison of calculated and measured mean and rms velocities.

Fig.3 at the top depicts calculated and measured sound pressure L_p for a far field monitor point ($x/D = 15, r/D = 30$), and at the bottom the spectra of total heat release rate $\dot{Q}_t$. In both cases with $\phi = 0.7$ (left) and $\phi = 0.9$ (right), L_p from TFC and DTF agree well with each other in the low frequency range ($f < 20$ Hz). With increasing frequency however, L_p from TFC is smaller than L_p from DTF, because a thicker flame is resolved by TFC-LES compared to DTF-LES, so that the resolved flame is less sensitive to high-frequency turbulent fluctuations. The TFC-LES shows better agreement with the experiment than DTF-LES in the range with $f < 100$ Hz. For higher frequencies, L_p is over-predicted by DTF-LES and under-predicted by TFC-LES. Corresponding to the results obtained for L_p, the spectra of $\dot{Q}_t$ are higher with DTF-LES than TFC-LES and the deviations between DTF and TFC are dependent on the frequency range. The results indicate a differently resolved flame response to turbulent fluctuations due to the use of different combustion models.

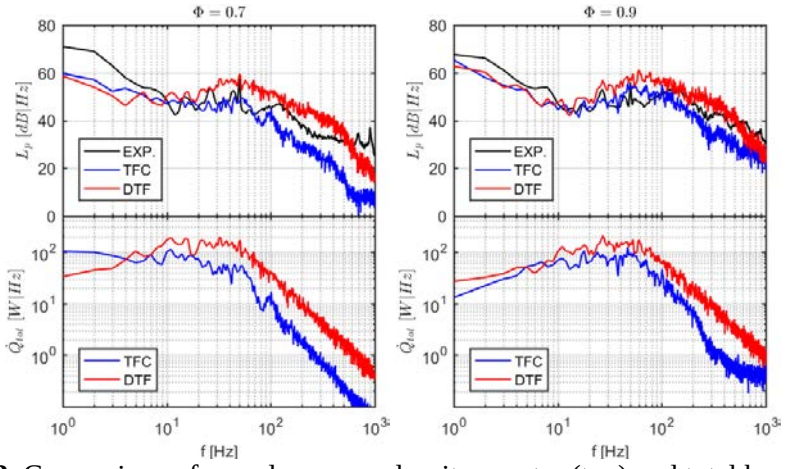

Figure 3. Comparison of sound pressure density spectra (top) and total heat release rate (bottom) calculated with TFC- and DTF-LES.

5. Conclusion

Two commonly used combustion models, the TFC and DTF approaches, are applied to LES of a turbulent premixed methane/air jet flame. Focus of this work lies on evaluating the ability of these combustion models to resolve the heat release rate and sound pressure in the spectral domain. The results reveal in which frequency range the heat release rate fluctuations can be correctly predicted by these models. As it has been elaborated in this work, the TFC shows better agreement with experiments than the DTF model in the low frequency range (see Fig.3), indicating that the DTF model is not always better suited than TFC for thermo-acoustic calculations.

Acknowledgements

The authors thank for the financial support by the German Research Council (DFG) through Research Units Bo 693/26-2 and DFG-PA920/12 "Combustion Noise". This work utilizes computational resources from the High Performance Computing Center Stuttgart (HLRS) and the Steinbuch Centre for Computing (SCC) at KIT.

References

[1] Dowling, A.P., Mahmoudi, Y., "Combustion noise", *Proc. Combust. Inst.* 35: 65-100 (2015).

[2] Bailly, C., Bogey, C., Candel, S., "Modelling of Sound Generation by Turbulent Reacting Flows", *Int. J. Aeroacoust.* 9: 461-490 (2010).

[3] Rajaram, R. Lieuwen, T., "Acoustic radiation from turbulent premixed flames", *J. Fluid Mech.* 637: 357-385 (2009).

[4] Zhang, F., Habisreuther, P., Bockhorn, H., Nawroth, H., Paschereit, C. O., "On Prediction of Combustion Generated Noise with the Turbulent Heat Release Rate ", *Acta. Acust. united with Ac*. 99: 940-951 (2013).

[5] Zhang, F., Habisreuther, P., Hettel, M., Bockhorn, H., "Numerical Computation of Combustion Induced Noise Using Compressible LES and Hybrid CFD/CAA Methods", *Acta. Acust. united with Ac*. 98: 120-134 (2012).

[6] Poinsot, T., Veynante, D., *Theoretical and numerical combustion*, Edwards Inc., Philadelphia, U.S.A., 2005.

[7] Peters, N., *Turbulent Combustion*, Cambridge University Press, Cambridge, U.K., 2000.

[8] Pitsch, H., "A consistent level set formulation for large-eddy simulation of premixed turbulent combustion", *Combust. Flame* 143: 587-598 (2005).

[9] Colin, O., Ducros, F., Veynante, D., Poinsot, T., "A thickened flame model for large eddy simulations of turbulent premixed combustion", *Phys. Fluids* 12: 1843-1863 (2000).

[10] Schmid, H., Habisreuther, P., Leuckel, W., "A model for calculating heat release in premixed turbulent flames", *Combust. Flame* 113: 79-91 (1998).

[11] Legier, J.P., Poinsot, T., Veynante, D., "Dynamically thickened flame LES model for premixed and non-premixed turbulent combustion", *Center for Turbulence Research, Proceedings of the Summer Program* 2000, p. 157.

[12] Nawroth, H., Paschereit, C.O., Zhang, F., Habisreuther, P., Bockhorn, H., "Flow Investigation and Acoustic Measurements of an Unconfined Turbulent Premixed Jet Flame", AIAA Paper, pp 2013-2459 (2013).

[13] Zhang, F., Zirwes, T., Nawroth, H., Habisreuther, P., Bockhorn, H., Paschereit, C.O., "Combustion-Generated Noise: An Environment-Related Issue for Future Combustion Systems", *Energy Technol*. 5: 1045-1054 (2017).

[14] OpenFOAM, The Open Source CFD Toolbox, User Guide (2014).

[15] Ferziger, J.H., Perić , M., *Computational methods for fluid dynamics*, Springer-Verlag Berlin Heidelberg, Germany, 2002.

[16] Smith, G., Golden, D.,Frenklach, M., Moriarty, N., Eiteneer, B., Goldenberg, M., Bowman, C., Hanson, R., Song, S., Gardiner, W., Lissianski, V., Qi, Z., Gri 3.0 reaction mechanism.

[17] Fröhlich, J., *Large Eddy Simulation turbulenter Strömungen*, Teubner Verlag, Germany, 2006.